Lab on a Chip

ROYAL SOCIETY OF CHEMISTRY

PAPER

View Article Online
View Journal

Cite this: DOI: 10.1039/d1lc00981h

Point-of-care blood coagulation assay enabled by printed circuit board-based digital microfluidics†

Donghao Li,‡[ab] Xinyu Liu,‡[abc] Yujuan Chai,‡[ab] Jieying Shan,[ab] Yihan Xie,[ab] Yong Liang,[c] Susu Huang,[d] Weidong Zheng[d] and Zida Li *[ab]

Received 1st November 2021,
Accepted 13th January 2022

DOI: 10.1039/d1lc00981h

rsc.li/loc

The monitoring of coagulation function has great implications in many clinical settings. However, existing coagulation assays are simplex, sample-consuming, and slow in turnaround, making them less suitable for point-of-care testing. In this work, we developed a novel blood coagulation assay that simultaneously assesses both the tendency of clotting and the stiffness of the resultant clot using printed circuit board (PCB)-based digital microfluidics. A drop of blood was actuated to move back and forth on the PCB electrode array, until the motion winded down as the blood coagulated and became thicker. The velocity tracing and the deformation of the clot were calculated *via* image analysis to reflect the coagulation progression and the clot stiffness, respectively. We investigated the effect of different hardware and biochemical settings on the assay results. To validate the assay, we performed assays on blood samples with hypo- and hyper-coagulability, and the results confirmed the assay's capability in distinguishing different blood samples. We then examined the correlation between the measured metrics in our assays and standard coagulation assays, namely prothrombin time and fibrinogen level, and the high correlation supported the clinical relevance of our assay. We envision that this method would serve as a powerful point-of-care coagulation testing method.

Introduction

Coagulation monitoring is critically important in the diagnosis of bleeding disorders and thrombotic diseases, such as von Willebrand disease, hemophilia, deep vein thrombosis, and disseminated intravascular coagulation.[1,2] Currently, clinical blood coagulation assays are mainly focused on the assessment of two different aspects. One aspect concerns the timing of the clotting and oftentimes adopts the strategy of endpoint testing, such as prothrombin time, activated partial thromboplastin time, and thrombin time. Another aspect concerns the biochemical functions and measures the concentrations of relevant biomarkers, such as clotting factors, fibrinogen, and D-dimer.[3]

Although these tests have been routinely used in clinical diagnostics, there are a few limitations. Firstly, though the mechanical properties of the resultant clots greatly affect the effectiveness of the hemostatic performance, this aspect is rarely gauged in routine coagulation assays. It has been shown that some patients exhibited excessive bleeding due to insufficient clot stability but coagulation tests appear normal.[4] Secondly, existing coagulation tests are mostly performed in clinical laboratories with a long turnaround time (>4 hours) and excessive sample consumption (~3 mL). Many clinical settings, such as critical care, perioperative care, and pediatric care, require short sample-to-result time for rapid decision making and/or low blood consumption. In addition, as multiple tests are normally ordered individually, cumulative blood consumption could add up to an unbearable level.[5] Though a few point-of-care coagulation devices, such as CoaguCheck, have been getting acceptance, the measurements are limited to the clotting tendency without accounting for the mechanical properties of the blood clot.

Point-of-care devices assessing the viscoelastic properties of whole blood, such as thromboelastography (TEG) and rotational thromboelastometry (ROTEM), provide methods to address these limitations and have been getting acceptance in clinical applications such as perioperative care[6] and sepsis treatment.[7] Nevertheless, these devices are costly, sample-consuming (~0.34 mL per test), and not easy to operate.[8]

[a] *Department of Biomedical Engineering, School of Medicine, Shenzhen University, Shenzhen 518060, China. E-mail: zidali@szu.edu.cn*
[b] *Guangdong Key Laboratory for Biomedical Measurements and Ultrasound Imaging, Department of Biomedical Engineering, School of Medicine, Shenzhen University, Shenzhen 518060, China*
[c] *Faculty of Information Technology, Collaborative Laboratory for Intelligent Science and Systems and State Key Laboratory of Quality Research in Chinese Medicines, Macau University of Science and Technology, Macao 999078, China*
[d] *Department of Laboratory Medicine, Shenzhen University General Hospital, Shenzhen 518055, China*

† Electronic supplementary information (ESI) available. See DOI: 10.1039/d1lc00981h

‡ Contributed equally.

Microfluidics provides promising tools to develop point-of-care blood assays given its advantages of small size, tiny sample consumption, and versatile prototyping.[9–11] To assess the rheology of blood samples and thus monitor coagulation function, studies using droplet microfluidics,[12] acoustic waves,[13–15] lasers,[16] micropost arrays,[17] mechanical resonance,[18] and electrical impedance[19–21] have been reported. Despite the potential that these methods have shown, the implementation relied on sophisticated instruments such as precision pumps, acoustic transducers, electric measuring instruments, and microscopes, limiting their practical applications.

This work aimed to develop a coagulation assay with the merits of low sample consumption, low cost, and fit for point-of-care testing. We implemented printed circuit board (PCB)-based digital microfluidics and developed a novel blood coagulation assay that simultaneously assesses both the clotting tendency and stiffness of the resultant clot. In the assay, a drop of blood sample is actuated by programmed voltages of the PCB electrode array and moves back and forth, as shown in Fig. 1a. As the blood clots and viscosity increases, the velocity decreases, and the temporal velocity curve reflects the clotting tendency. As the clot stops moving, it is subject to stretching due to the voltage on the electrode array, and its deformation reflects the clot stiffness. The motion and length of the blood drops are calculated using image analysis to derive the clotting tendency and clot deformability. We investigated the effect of hardware settings, namely the voltage magnitude and refresh rate, and biochemical settings, namely the $CaCl_2$ concentration and temperature, on the measurement results. To show the capability of this assay to distinguish samples with varied coagulation functions, we performed the assay on blood samples spiked with a pro- and anti-coagulant, and the results agreed with predictions. We further examined the correlation between our measurement and standard tests of prothrombin time and fibrinogen level, showing that our assay possessed good clinical relevance. This assay offers multiplex measurements of both the clotting time and clot stiffness, providing a comprehensive assessment of coagulation function. In addition, the great manufacturability of the PCB makes the assay economical. Compared to other reported studies (Table S1†), the multiplex measurements, low cost, and low blood consumption gave this assay great potential for applications in point-of-care coagulation testing.

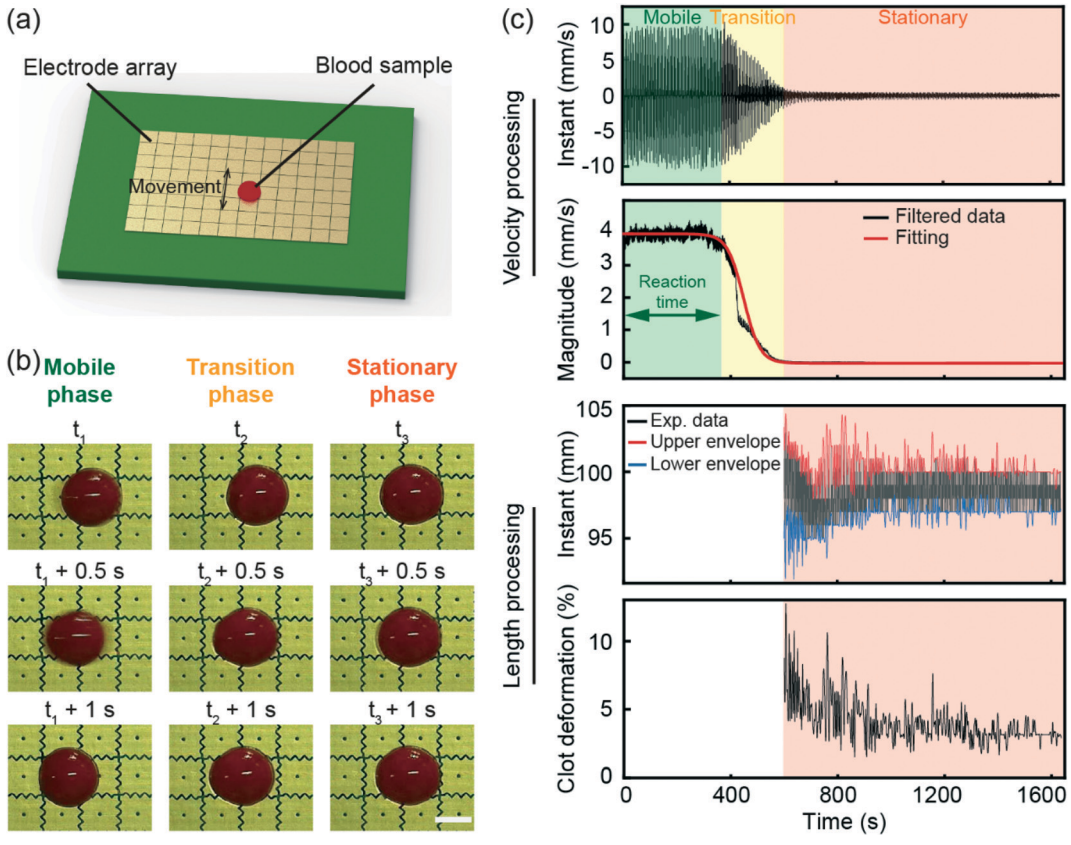

Fig. 1 Overview of the blood coagulation assay enabled by the printed circuit board-based digital microfluidics. (a) Schematic showing the assay principle. The electrode array is programmed to drive a drop of blood moving back and forth. As the blood coagulates and becomes more viscous, the velocity magnitude decreases until the blood drop no longer shows motion. Afterward, the formed clot is stretched *in situ*, and the deformation is measured to report the stiffness of the resultant clots. (b) Micrographs showing the blood drop at different time points into the assay. Scale bar, 2 mm. (c) Processing steps of the velocity and length of the blood drop to give the velocity magnitude and clot deformability.

Methods

Device design and experimental setup

The design of the digital microfluidic platform was adapted from OpenDrop, an open-source digital microfluidics platform for research purposes.[22] The platform mainly consisted of a microcontroller unit, a high voltage unit, and an electrode array, as shown in Fig. S2.† The microcontroller unit generated serial control signals, which were converted to parallel signals by the high voltage unit and supplied to the electrode array. High voltage was generated by a function generator (Model AFG022, Tektronix Inc.), amplified to 230 V by a voltage amplifier (Model ATA-7020, Aigtek Inc.), and supplied to the high voltage unit. The actuating signals (high voltage) were updated every 1 second. The fabrication of the printed circuit boards was outsourced to a PCB prototype company (Shenzhen Jialichuang Technology Development Co.).

The electrode array adopted an open configuration and was mainly composed of square electrodes (2.5 mm × 2.5 mm). A sealing film (Parafilm, Bemis Company) was stretched by 2–3-fold, resulting in a thin film of about 50 μm thick, and adhered to the electrode array to serve as the dielectric layer. Silicone oil with a viscosity of 10 cSt (S104742, Aladdin Biochemical Technology Co.) was then spread on top of the sealing film to improve the hydrophobicity. Software on Windows was designed and implemented using C# to interface with the microcontroller and program the voltage sequences. Droplet movements on the electrode array were monitored using a digital microscope (Dino-Lite AM4113T, AnMo Electronics Corp.).

Blood specimen and assays

Under a protocol approved by the Institutional Review Board in Health Science Center at Shenzhen University, blood specimens were collected from human volunteers at Shenzhen University General Hospital after obtaining informed consent. Blood specimens were collected using blue-top vacutainer tubes containing 3.8% sodium citrate (Improvacuter, Improve Medical) and tested within 4 hours after blood draw. The fibrinogen level (FIB) and prothrombin time (PT) were tested using a commercial platform (CS-5100 Hemostasis System, Sysmex Corp.) at Shenzhen University General Hospital using corresponding reagents (Dade Thrombin Reagent, B4233-27, Siemens AG; Thromborel S Reagent, OUHP49, Siemens AG).

Unless otherwise mentioned, the digital microfluidics-based coagulation assays were performed using re-calcified citrated whole blood at 25 °C in an air-conditioned room. In a typical assay, 17 μL of citrated blood sample was placed on the electrode array, before 1 μL of 0.2 M $CaCl_2$ (C3306, Sigma-Aldrich Co.) was supplemented into the blood drop to neutralize the citrate and trigger blood coagulation. A lid made from acrylic was then placed on the electrode array to alleviate evaporation. Actuating voltage with the designed pattern and sequence was then supplied, and video capturing was immediately started at a frame rate of 15 frames per second. Experiments typically lasted for 20 minutes until the blood drop stopped showing obvious movement. During the experiment, the device was kept in a relatively isolated place to minimize external lighting disturbance and ensure a consistent lighting condition.

Blood samples with regular clotting function spiked with kaolin (final concentration of 5 mg mL^{-1}; K915603, Shanghai Macklin Biochemical Co.) and heparin (final concentration of 8 U mL^{-1}; H811552, Shanghai Macklin Biochemical Co.) were used as mock clinical samples with hyper- and hypo-coagulation functions, respectively, to validate the assay. Both samples were incubated at room temperature for 1 hour before being loaded into the device. Coagulation assays at 37 °C were performed by placing the PCB electrode array in a laboratory-made acrylic box equipped with a temperature controller (TC-05B, Xifa Electronics) and a strip heater (Model 60 227, Baohing Electric Wire & Cable Co.).

Image analysis and data processing

The captured videos were analyzed using Droplet Morphometry and Velocimetry (DMV) software[23] and a lab-made program, both coded in MATLAB (MathWorks, Inc.), to calculate the velocity and length of drops, respectively. In the DMV software, a frame of the empty PCB electrode array was selected or synthesized as the background, and each frame was subtracted from the background, before edge detection, small object removal, morphological close and fill, and shape detection were performed on the resultant image, as shown in Fig. S3.† The scale to convert image pixels to physical distance was obtained based on the designed dimension of the electrode (2.5 mm by 2.5 mm). The area and location of blood droplets in each frame were then calculated, outputted, and used for object matching between frames. Eventually, the time series of the velocity of each blood drop were exported for further signal processing. To obtain the magnitude of the fluctuant velocity and area, a 4th order high-pass Butterworth filter with a cutoff frequency of 0.8 Hz was implemented in MATLAB to obtain the high-frequency components, and the variation of a moving window of 200 data points was computed as the velocity magnitude. The velocity, v, as a function of time, t, was then fitted into a Boltzmann sigmoid function in the format of

$$v(t) = \frac{V_i - V_f}{1 + e^{(t-t_0)/\tau}} + V_f$$

where V_i is the initial velocity, V_f is the final velocity (normally 0), t_0 is the center time of the velocity descending period, and τ is the time constant. We defined reaction time as the time the blood drop took to start slowing down, marked as a velocity of $0.99V_i$. The blood drop then gradually came to a standstill, marked as a velocity of $0.01V_i$. After that, to calculate the length and thus the deformation of the clot upon actuation, we implemented a different image analysis pipeline (Fig. S4†). Briefly, the original image in RGB color space was converted to CIELAB color space, and the a* dimension was extracted and

converted to a grayscale image. Afterward, a series of morphological operations, including binarization, edge detection, and binary fill holes, were performed, and the length in the stretching direction was defined as the drop length. A code sample is included in the ESI.† To obtain the clot deformation, the upper envelope and lower envelope of the temporal curve of droplet length were first calculated, and the ratio of their difference to the lower envelope was calculated as the instant strain. The temporal mean of the strain was defined as the clot deformation to indicate the clot deformability. To investigate the clinical relevance of our method to standard coagulation tests, we analyzed the correlation between reaction time and prothrombin time and the correlation between the clot deformation and fibrinogen level. A two-sided two-sample *t*-test was adopted for hypothesis testing, and significance was defined as $p \leq 0.05$. Origin (OriginLab Corporation) was used for statistical analysis.

Results

Overview of the assay

The coagulation assay was performed by electrically driving a blood drop to move back and forth on an electrode array, based on the effect of electrowetting on dielectrics, and simultaneously monitoring the motion of the blood drop (Fig. 1a and S1; Video S1†). A typical assay was started by dispensing a blood drop (~17 μL) on the electrode array with $CaCl_2$ immediately supplemented to initiate the coagulation reaction. Initially, the blood was less viscous, and the blood drop moved smoothly, as shown in Fig. 1b and Video S2.† We termed this stage the mobile phase. After a few minutes, the viscosity started increasing, and the velocity magnitude gradually decreased until the blood drop became a clot and came to a halt. The temporal development of velocity provided the timing information of the coagulation reaction and indicated the clotting tendency. Afterwards, though the blood clot essentially showed no displacement, it was steadily actuated and stretched by the electric signal, providing the opportunity to gauge the deformability of the resultant clot (Fig. 1b). We termed the final stage the stationary phase and the middle stage the transition phase.

The assay was implemented on a printed circuit board (PCB)-based digital microfluidics platform,[22] and the movement of the blood drop was recorded by a camera (Fig. S2†). We performed image analysis to obtain the instant velocity of the blood drop (Fig. S3†). As shown in Fig. 1c, the instant velocity was in a pulsating manner, and the velocity magnitude was relatively constant in the mobile phase, winding down in the transition phase, and nearly zero in the stationary phase. To obtain the velocity magnitude, we filtered the signal and calculated the moving variance. The time series of velocity magnitude was then fitted into a sigmoid function, and 1% change was adopted to cut off the three phases. The duration of the mobile phase was defined as reaction time to indicate the clotting tendency, which was essentially the time it took the blood to start clotting.

In the stationary phase, the blood drop formed a clot and stopped moving, but it was subject to stretching induced by the voltage signals. To characterize the deformation and thus the stiffness of the resultant clot, we first analyzed the instant length of the clot by means of image analysis (Fig. 1c and S4†). The difference between the upper and the lower envelopes was divided by the lower envelopes to calculate the clot deformation at different time points. The temporal mean was reported as the clot deformation under the influence of the voltage to indicate the deformability of the clot.

Characterization of the assay design

We first aimed to characterize the assay design by investigating how different parameters affected the assay results. Parameters mainly came from two different sources, namely the hardware setting of the PCB digital microfluidics and the biochemical setting of the assay.

Regarding the hardware setting, the voltage magnitude of the electrode and the refresh rate of the voltage signal are the major parameters that affect the measurements. The voltage magnitude affects the strength of the electric field and thus the driving force of the drop movement, which could have implications on the coagulation reaction. We systematically adjusted the voltage magnitude and performed the coagulation assay. Results showed that blood drops were not able to move on the electrode array when the voltage was below 200 V due to insufficient driving force. Above 200 V, the velocity magnitude increased as the voltage was set higher (Fig. 2a), which was likely due to the higher voltage providing a more considerable EWOD effect. Nevertheless, the voltage value did not show a significant impact on the progression of the coagulation assay and the deformation of the resultant clots, as suggested by the calculated reaction times and clot deformation that were not significantly different among each voltage condition (Fig. 2b and c).

The refresh rate of the electrode voltage determined the duration of each voltage signal and thus the duration of each displacement of blood drops. At a higher refresh rate, the blood drops would likely move faster and thus experience a higher shear rate, which could affect the progression of the coagulation reaction and the stiffness of the resultant clot.[24] We set the refresh rate at 0.5, 1, 2, and 4 Hz, respectively, and performed the coagulation assay. As the voltages switched faster, we saw an increase in the velocity magnitude as we anticipated (Fig. 2d). The reaction times calculated from each refresh rate were not significantly different, suggesting that the clotting tendency was likely not significantly affected (Fig. 2e). However, we observed an increase in the clot deformations as we increased the refresh rate (Fig. 2f). For example, the clot deformation was (3.9 ± 0.9)% at a refresh rate of 0.5 Hz, which was significantly smaller than (5.6 ± 0.6)% at 4 Hz. These results suggested that the assay results likely had weak dependence on the setting of the voltage and refresh rate of the voltage.

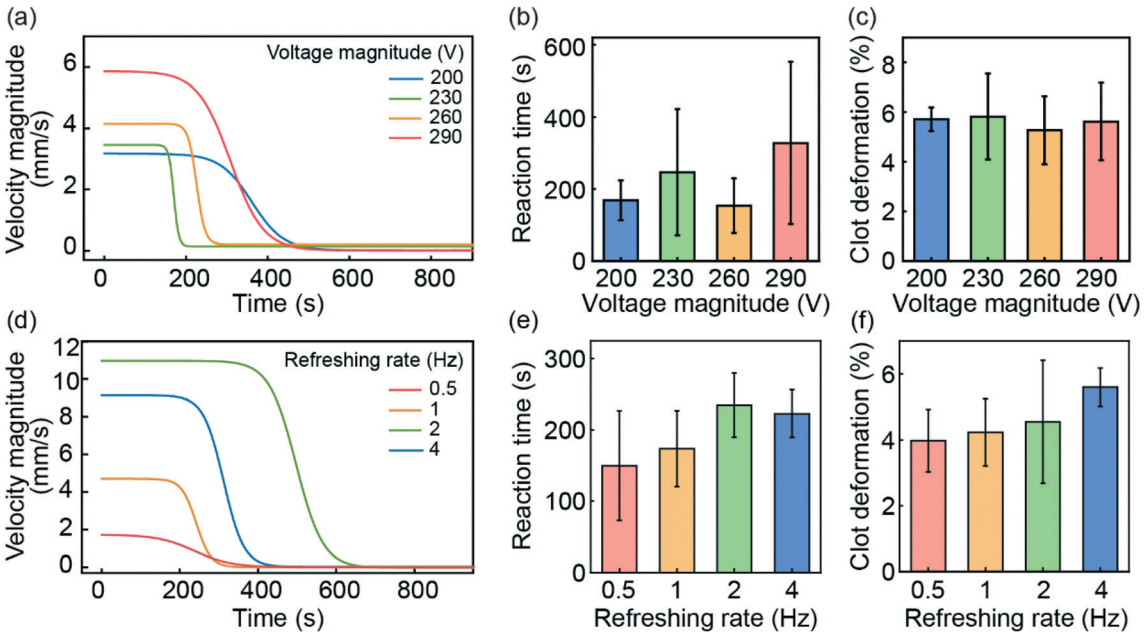

Fig. 2 (a–c) Effect of the voltage magnitude on assay results. (a) Representative temporal velocity magnitudes of the blood drops when the voltage was set at 200, 230, 260, and 290 V. (b) Bar plot of reaction time as a function of the voltage magnitude. (c) Bar plot of clot deformation as a function of the voltage magnitude. Data represent mean ± SD with n = 3. (d–f) Effect of the refresh rate on assay results. (d) Representative temporal velocity magnitude of blood drops when the refresh rate was set at 0.5, 1, 2, and 4 Hz. (e) Bar plot of reaction time as a function of the refresh rate. (f) Bar plot of clot deformation as a function of the refresh rate. Data represent mean ± SD with n = 3.

Regarding the biochemical setting of the assay, the $CaCl_2$ concentration and assay temperature are the parameters that directly affect the measurements. We examined the effect of $CaCl_2$ concentration by adding 0, 0.1, and 0.2 M $CaCl_2$ solution, respectively, at a volume-to-volume ratio of 17 : 1 and performed the assays. When $CaCl_2$ was absent, the citrated blood moved continuously on the electrode array without coagulation (Fig. 3a). The addition of 0.1 M $CaCl_2$ led to velocity downswing at about 170 s into the assay, showing that the disruption in blood drop motion was indeed induced by blood clotting. In comparison, as shown in Fig. 3b, the addition of 0.2 M $CaCl_2$ triggered a later onset of velocity

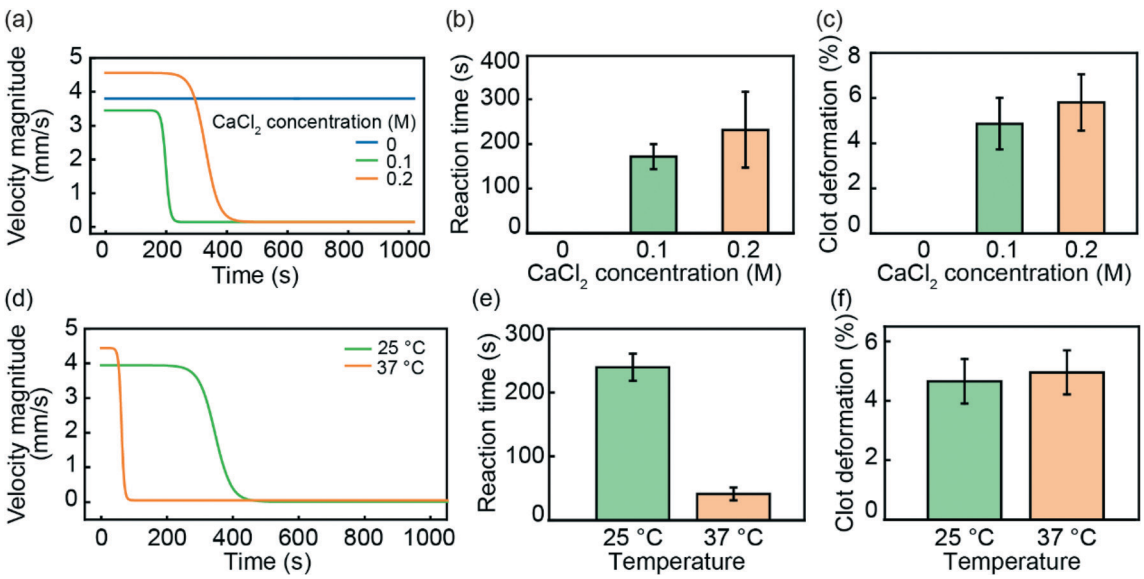

Fig. 3 (a–c) Effect of the $CaCl_2$ concentration on assay results. (a) Representative temporal velocity magnitudes of the blood drops using samples recalcified with 0, 0.1, and 0.2 M $CaCl_2$. (b) Bar plot of reaction time as a function of $CaCl_2$ concentration. (c) Bar plot of strain as a function of $CaCl_2$ concentration. Data represent mean ± SD with n = 3. (d–f) Effect of assay temperature on the assay results. (d) Representative temporal velocity magnitude of blood drops measured at 25 °C and 37 °C. (e) Bar plot of reaction time as a function of assay temperature. (f) Bar plot of strain as a function of assay temperature. Data represent mean ± SD with n = 3.

downswing with a reaction time of about 230 s, which agreed with reported studies.[25] In terms of deformability, groups of both 0.1 M and 0.2 M showed about 5% of clot deformation with no statistically significant difference (Fig. 3c). These results showed that the re-calcification should be standardized to guarantee repeatable measurements.

Temperature affects enzyme activities and thus could pose a great impact on the coagulation reaction. Room temperature and body temperature are the two temperatures that are most clinically relevant. We performed the assay at both 25 °C and 37 °C, representing room temperature and body temperature, respectively. As anticipated, coagulation progressed much faster at 37 °C than 25 °C, with a measured reaction time of 41.3 ± 10.1 s, significantly smaller than 239.7 ± 21.4 s at 25 °C (Fig. 3d and e). Nevertheless, the tracing of the velocity magnitude showed similar dynamics, suggesting that low temperature only delayed the reaction without altering the trending. In contrast, the clot deformability was not significantly different, with the calculated clot deformation being (5.0 ± 0.7)% at 37 °C and (4.6 ± 0.7)% at 25 °C (Fig. 3f). These results suggested that assays could be conducted at 25 °C to reduce the cost of temperature control, on the tradeoff of prolonged assay time.

Performance validation of the assay

To validate the capability of this assay to distinguish blood samples with hyper- and hypo-coagulability, we pre-treated baseline blood samples with either a procoagulant, namely kaolin (working concentration of 5 mg mL^{-1}), or an anticoagulant, namely heparin (working concentration of 8 U mL^{-1}), to serve as mock clinical samples. The results showed that the blood sample pre-treated with kaolin demonstrated an accelerated clotting process with a reaction time of 53.7 ± 28.0 s, which was significantly larger than 171.5 ± 51.6 s in the control group (Fig. 4a and b). Despite the altered coagulation progression induced by kaolin treatment, the resultant clots showed similar deformability, with a clot deformation of (7.0 ± 1.2)% in the kaolin-treated group and (9.0 ± 4.8)% in the control group (Fig. 4c). These results suggested that though kaolin accelerated the clot formation, it had little effect on the clot stability, which agreed with the reported findings.[26] In contrast, in heparin-treated samples, the blood drop moved continuously without showing deceleration or forming a clot throughout the assay, which agreed with the strong anti-coagulating effect of heparin.

To further validate the clinical relevance of this assay, we analyzed the correlation between our measurements and standard coagulation tests, namely prothrombin time and fibrinogen level. Prothrombin time assesses the clotting tendency of blood samples, which should be correlated to the reaction time measured in our assays. Fibrinogen levels measure the fibrinogen concentration in the blood sample and affect the stability of the resultant clots. Higher fibrinogen levels reportedly resulted in enhanced clot stability and stiffness.[27] Therefore, the measured clot deformation in our assay is supposed to be negatively correlated to fibrinogen levels. We tested eleven patient samples using our assay and simultaneously measured the prothrombin time and fibrinogen level using standard instruments. The calculated reaction time from our assays showed a strong positive correlation with prothrombin time, as shown in Fig. 5a, with a Pearson's correlation coefficient of 0.89 ($P < 0.01$), suggesting that the reaction time measured in our assay could potentially serve as an indicator of the coagulation tendency. The calculated clot deformation was negatively correlated with the fibrinogen level, with a Pearson's correlation coefficient of −0.89 ($P < 0.01$), as shown in Fig. 5b. The strong correlation between the measured clot deformation and fibrinogen level suggested that the clot deformation measured in our assay could indeed represent the mechanical stiffness of the formed clot. These results showed that our assay, along with the derived metrics of reaction time and clot deformation, had reasonable clinical relevance.

Discussion and conclusions

In this work, we presented the design of a blood coagulation assay using a printed circuit board (PCB)-based digital

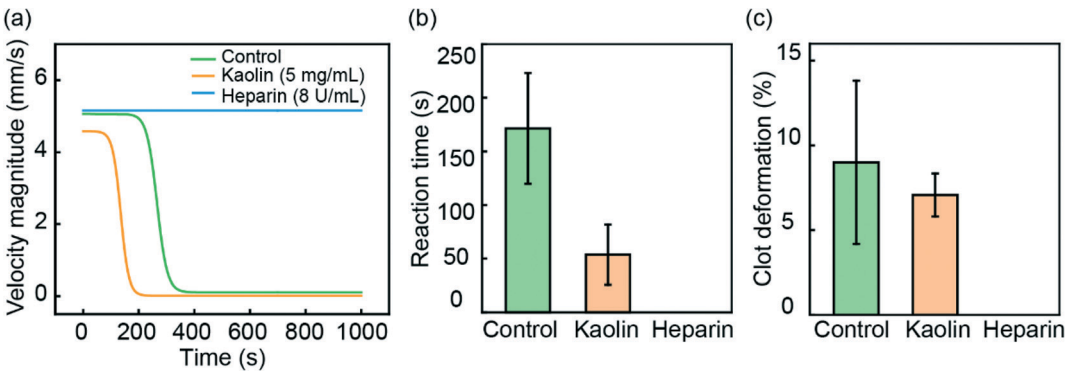

Fig. 4 Effect of pro- and anti-coagulants on the assay results. (a) Temporal velocity magnitude of blood drops treated with a procoagulant, namely kaolin, and an anticoagulant, namely heparin. (b) Bar plot of reaction time as a function of reagent treatments. (c) Bar plot of strain as a function of reagent treatments.

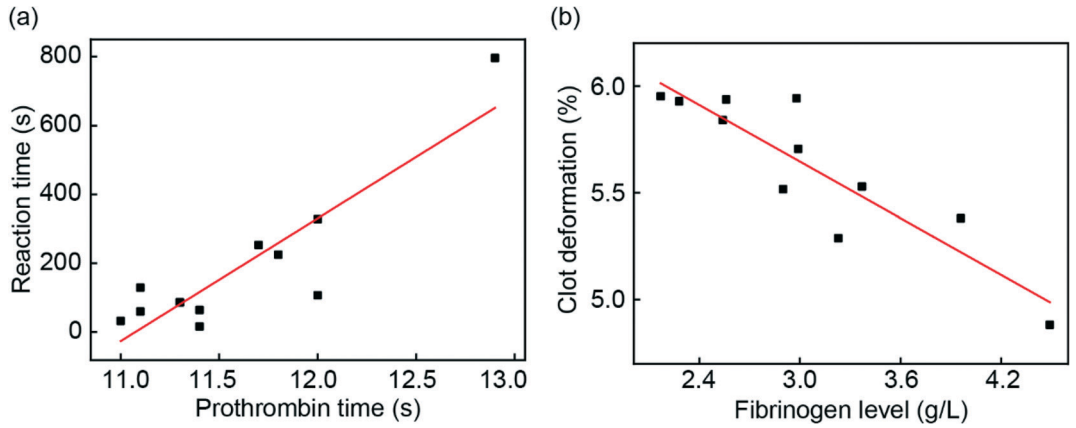

Fig. 5 Correlation between the results from this assay and standard assays, namely prothrombin time and fibrinogen level. (a) Correlation between the measured reaction time and prothrombin time. Pearson's correlation coefficient was calculated to be 0.89 with $P < 0.01$. (b) Correlation between the measured clot deformation and fibrinogen level. Pearson's correlation coefficient was calculated to be −0.89 with $P < 0.01$.

microfluidics platform. Unlike many other coagulation assays that assess only one aspect of coagulation, this assay provided information on both the clotting tendency and stiffness of the resultant clot. In addition, the blood drop was constantly exposed to shear force during the assay, offering a more physiologically relevant assay condition. Finally, given the highly standardized PCB manufacturing, the marginal cost per assay could be as low as one US dollar. These merits could potentially make this assay a great point-of-care blood coagulation testing tool.

Nevertheless, the current form of the digital microfluidics platform requires a voltage of at least 230 V to operate, which could be problematic in some settings. Future work shall be devoted to improving the processing of the dielectric layer and hydrophobic layer to reduce the working voltage. In addition, by integrating an on-board voltage amplifier into the high voltage unit, the external voltage amplifier could be eliminated, making the device more compact and portable.

Author contributions

Z. L. conceptualized the project and designed the experiments. X. L., J. S., and Y. X. adapted the design of the digital microfluidics platform, implemented the hardware, and developed the accompanying software. S. H. and W. Z. collected the blood samples. D. L. performed the experiments. D. L., Y. C., and Z. L. analyzed the data. D. L., Y. C., and Z. L. wrote the manuscript. All the authors contributed to the manuscript.

Conflicts of interest

There are no conflicts to declare.

Acknowledgements

The authors thank Prof. Amar S. Basu from Wayne State University for providing the access to the DMV software and Prof. Gan Huang from Shenzhen University for the assistance on signal processing. This work was supported by the Natural Science Foundation of Guangdong Province (2019A1515012010), Shenzhen Overseas Talent Program, and Shenzhen University Student Research Grants (315-470833 and 860-1021991).

References

1 S. M. Bates and J. I. Weitz, Coagulation Assays, *Circulation*, 2005, **112**(4), e53–e60.
2 Y. L. Chee, J. C. Crawford, H. G. Watson and M. Greaves, Guidelines on the assessment of bleeding risk prior to surgery or invasive procedures. British Committee for Standards in Haematology, *Br. J. Haematol.*, 2008, **140**(5), 496–504.
3 W. E. Winter, S. D. Flax and N. S. Harris, Coagulation Testing in the Core Laboratory, *Lab. Med.*, 2017, **48**(4), 295–313.
4 D. R. Myers, Y. Qiu, M. E. Fay, M. Tennenbaum, D. Chester, J. Cuadrado, Y. Sakurai, J. Baek, R. Tran, J. C. Ciciliano, B. Ahn, R. G. Mannino, S. T. Bunting, C. Bennett, M. Briones, A. Fernandez-Nieves, M. L. Smith, A. C. Brown, T. Sulchek and W. A. Lam, Single-platelet nanomechanics measured by high-throughput cytometry, *Nat. Mater.*, 2017, **16**(2), 230–235.
5 S. M. Emani, Novel Coagulation Analyzers in Development: A Glimpse toward the Future of Microfluidics, *Semin. Thromb. Hemostasis*, 2019, **45**(3), 302–307.
6 R. B. Hawkins, S. L. Raymond, T. Hartjes, P. A. Efron, S. D. Larson, K. A. Andreoni and E. M. Thomas, Review: The Perioperative Use of Thromboelastography for Liver Transplant Patients, *Transplant. Proc.*, 2018, **50**(10), 3552–3558.
7 N. Haase, S. R. Ostrowski, J. Wetterslev, T. Lange, M. H. Møller, H. Tousi, M. Steensen, F. Pott, P. Søe-Jensen, J. Nielsen, P. B. Hjortrup, P. I. Johansson and A. Perner,

Thromboelastography in patients with severe sepsis: a prospective cohort study, *Intensive Care Med.*, 2015, **41**(1), 77–85.

8 M. T. Ganter and C. K. Hofer, Coagulation Monitoring: Current Techniques and Clinical Use of Viscoelastic Point-of-Care Coagulation Devices, *Anesth. Analg.*, 2008, **106**(5), 1366–1375.

9 X. Li, W. Chen, Z. Li, L. Li, H. Gu and J. Fu, Emerging microengineered tools for functional analysis and phenotyping of blood cells, *Trends Biotechnol.*, 2014, **32**(11), 586–594.

10 L. F. Harris and A. J. Killard, Microfluidics in coagulation monitoring devices: a mini review, *Anal. Methods*, 2018, **10**(30), 3714–3719.

11 M. Mohammadi Aria, A. Erten and O. Yalcin, Technology Advancements in Blood Coagulation Measurements for Point-of-Care Diagnostic Testing, *Front. Bioeng. Biotechnol.*, 2019, **7**, 395.

12 S. E. Mena, Y. Li, J. McCormick, B. McCracken, C. Colmenero, K. Ward and M. A. Burns, A droplet-based microfluidic viscometer for the measurement of blood coagulation, *Biomicrofluidics*, 2020, **14**(1), 014109.

13 J. Nam, H. Choi, J. Y. Kim, W. Jang and C. S. Lim, Lamb wave-based blood coagulation test, *Sens. Actuators, B*, 2018, **263**, 190–195.

14 X. Chen, M. Wang and G. Zhao, Point-of-Care Assessment of Hemostasis with a Love-Mode Surface Acoustic Wave Sensor, *ACS Sens.*, 2020, **5**(1), 282–291.

15 W. Xu, J. Appel and J. Chae, Real-time monitoring of whole blood coagulation using a microfabricated contour-mode film bulk acoustic resonator, *J. Microelectromech. Syst.*, 2012, **21**(2), 302–307.

16 S. K. Nadkarni, Comprehensive Coagulation Profiling at the Point-of-Care Using a Novel Laser-Based Approach, *Semin. Thromb. Hemostasis*, 2019, **45**(3), 264–274.

17 R. M. Judith, J. K. Fisher, R. C. Spero, B. L. Fiser, A. Turner, B. Oberhardt, R. Taylor, M. R. Falvo and R. Superfine, Micro-elastometry on whole blood clots using actuated surface-attached posts (ASAPs), *Lab Chip*, 2015, **15**(5), 1385–1393.

18 G. Erdoes, H. Schloer, B. Eberle and M. Nagler, Next generation viscoelasticity assays in cardiothoracic surgery: Feasibility of the TEG6s system, *PLoS One*, 2018, **13**(12), e0209360.

19 L. Duan, X. Lv, Q. He, X. Ji, M. Sun, Y. Yang, Z. Ji and Y. Xie, Geometry-on-demand fabrication of conductive microstructures by photoetching and application in hemostasis assessment, *Biosens. Bioelectron.*, 2020, **150**, 111886.

20 D. Maji, M. A. Suster, E. Kucukal, U. D. Sekhon, A. S. Gupta, U. A. Gurkan, E. X. Stavrou and P. Mohseni, ClotChip: A Microfluidic Dielectric Sensor for Point-of-Care Assessment of Hemostasis, *IEEE Trans. Biomed. Circuits Syst.*, 2017, **11**(6), 1459–1469.

21 B. Ramaswamy, Y.-T. T. Yeh and S.-Y. Zheng, Microfluidic device and system for point-of-care blood coagulation measurement based on electrical impedance sensing, *Sens. Actuators, B*, 2013, **180**, 21–27.

22 M. Alistar and U. Gaudenz, OpenDrop: An Integrated Do-It-Yourself Platform for Personal Use of Biochips, *Bioengineering*, 2017, **4**(2), 45.

23 A. S. Basu, Droplet morphometry and velocimetry (DMV): a video processing software for time-resolved, label-free tracking of droplet parameters, *Lab Chip*, 2013, **13**(10), 1892–1901.

24 L. H. Ting, S. Feghhi, N. Taparia, A. O. Smith, A. Karchin, E. Lim, A. S. John, X. Wang, T. Rue and N. J. White, Contractile forces in platelet aggregates under microfluidic shear gradients reflect platelet inhibition and bleeding risk, *Nat. Commun.*, 2019, **10**(1), 1204.

25 C. S. Greenberg, J. P. Adams, P. E. Mullen and J. A. Koepke, The Effect of Calcium Ions on the Activated Partial Thromboplastin Time of Heparinized Plasma, *Am. J. Clin. Pathol.*, 1986, **86**(4), 484–489.

26 F. J. Castellino, Z. Liang, P. K. Davis, R. D. Balsara, H. Musunuru, D. L. Donahue, D. L. Smith, M. J. Sandoval-Cooper, V. A. Ploplis and M. Walsh, Abnormal Whole Blood Thrombi in Humans with Inherited Platelet Receptor Defects, *PLoS One*, 2012, **7**(12), e52878.

27 C. E. Dempfle, T. Kälsch, E. Elmas, N. Suvajac, T. Lücke, E. Münch and M. Borggrefe, Impact of fibrinogen concentration in severely ill patients on mechanical properties of whole blood clots, *Blood Coagulation Fibrinolysis*, 2008, **19**(8), 765–770.

